EI SEVIER

Contents lists available at ScienceDirect

Science of the Total Environment

journal homepage: www.elsevier.com/locate/scitotenv



Development of statistical models for estimating daily nitrate load in Iowa



Jessica R. Ayers a,*, Gabriele Villarini a, Keith Schilling a,b, Christopher Jones a,b

- ^a IIHR—Hydroscience & Engineering, The University of Iowa, Iowa City, Iowa, USA
- ^b Iowa Geological Survey, The University of Iowa, Iowa City, Iowa, USA

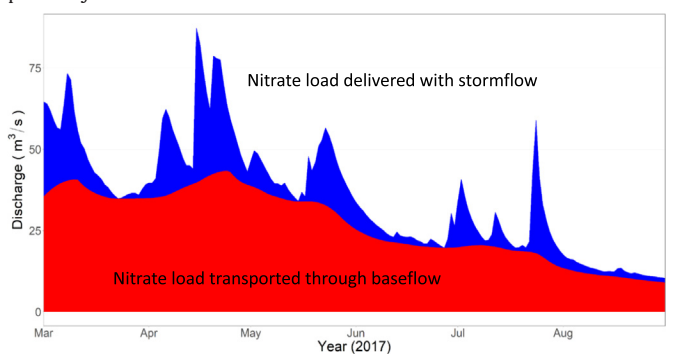
HIGHLIGHTS

Four models compared baseflow and stormflow discharge to nitrate loads in eight lowa watersheds.

- The baseflow-stormflow models highlight the importance of separating out streamflow.
- Baseflow was better at predicting smaller nitrate loads while stormflow captured peak loads.

GRAPHICAL ABSTRACT

There is an ongoing need to increase our understanding of the sources and timing of stream nitrate loads across agricultural watersheds in Iowa as water quality improvement strategies are implemented. The goal of this study was to model the relationship between nitrate load and the two components of streamflow (i.e., baseflow and stormflow) to quantify in-stream nitrate patterns and develop a new method for estimating loads on days when monitoring data are not available. We analyzed eight watersheds in Iowa that had long-term water quality data where grab samples have been collected from 1987 to 2019. Four regression models were developed that related daily nitrate load to daily baseflow, stormflow, and streamflow discharge. The first model considered baseflow as a predictor, the second model used stormflow, the third model included both baseflow and stormflow as two different covariates, and the final model used total streamflow (unseparated). For all eight watersheds, the baseflow-stormflow models had the highest correlation coefficients, which indicates that both components are necessary and together improve nitrate load estimates. While baseflow models estimated lower nitrate loads better, stormflow models captured the variability associated with larger loads. In addition, streamflow models tended to overestimate large nitrate loads. This simple modeling framework can be used to calculate daily, monthly and annual nitrate loads. Delineating nitrate loads between stormflow and baseflow can help identify differences in nitrate sources for nutrient reduction and remediation.



ARTICLE INFO

Article history: Received 31 December 2020 Received in revised form 14 March 2021 Accepted 17 March 2021 Available online 22 March 2021

Editor: Jose Julio Ortega-Calvo

$A\ B\ S\ T\ R\ A\ C\ T$

There is an ongoing need to increase our understanding of the sources and timing of stream nitrate loads across agricultural watersheds in Iowa as water quality improvement strategies are implemented. The goal of this study was to model the relationship between nitrate load and the two components of streamflow (i.e., baseflow and stormflow) to quantify in-stream nitrate patterns and develop a new method for estimating loads on days when monitoring data are not available. We analyzed eight watersheds in Iowa that had long-term water quality data where grab samples have been collected from 1987 to 2019. Four regression models were developed that related daily nitrate load to daily baseflow, stormflow, and streamflow discharge. The first model considered baseflow as a predictor, the second model used stormflow, the third model included both baseflow and

^{*} Corresponding author. E-mail address: jessica-ayers@uiowa.edu (J.R. Ayers).

Keywords: Nitrate load Discharge Stormflow Baseflow Statistical modeling stormflow as two different covariates, and the final model used total streamflow (unseparated). For all eight watersheds, the baseflowstormflow models had the highest correlation coefficients, which indicates that both components are necessary and together improve nitrate load estimates. While baseflow models estimated lower nitrate loads better, stormflow models captured the variability associated with larger loads. In addition, streamflow models tended to overestimate large nitrate loads. This simple modeling framework can be used to calculate daily, monthly and annual nitrate loads. Delineating nitrate loads between stormflow and baseflow can help identify differences in nitrate sources for nutrient reduction and remediation.

© 2021 Published by Elsevier B.V.

1. Introduction

Nitrate-nitrogen (nitrate) discharged to streams degrades drinking water supplies around the world. Excess nitrate in streams and rivers has resulted in large-scale eutrophication in receiving and downstream waters (Buda and DeWalle, 2009; Wherry et al., 2021). For example, in the U.S. Cornbelt state of Iowa, nitrate export is a major cause for hypoxia in the Gulf of Mexico (Jones et al., 2018a; US EPA, 2015). Nitrate originates from the application of commercial nitrogen fertilizers, livestock manure, and the fixation and mineralization of soil nitrogen (e.g., Schilling and Lutz, 2004). Although the sources and environmental consequences of nitrate are well known, the discharge-nitrate relationship is not fully understood which can confound efforts to link improvements from nutrient reduction programs (e.g., Jones et al., 2018a, 2018b; Schilling et al., 2017; Schubert et al., 2004; Van Meter and Basu, 2017; Zimmer et al., 2019). Accurately characterizing this relationship can increase the effectiveness of reduction strategies and bring accountability to public funds spent on water quality improvements.

Water quality monitoring programs are often limited because funding is inadequate and field samples are costly to obtain. As a result, studies usually rely on small-scale samples or generalized watersheds models and programs are conducted on a short time scale (~a few months to five years) (Schilling and Thompson, 2000). When data are collected infrequently, it is a challenge to obtain a complete picture of nitrate concentrations and loads. To acquire data between grab sample observations, concentrations must be estimated, subjecting loads to sources of error and uncertainty (Guo et al., 2002; Stenback et al., 2011). Some studies have run physical models to fill in data gaps (Drake et al., 2018; Hansen et al., 2007; Husic et al., 2019; Nikolaidis et al., 2013), but these models are complex to develop and implement on a large scale. In many cases, linear interpolation is used to fill in missing data for nitrate concentration (e.g., Goolsby et al., 2000; Jones et al., 2018a, 2018b; Kelly et al., 2015; Lee et al., 2016; Miller et al., 2017; Schilling and Lutz, 2004; Zamyadi et al., 2007); however, this technique is not without limitations. For example, it can be difficult to capture long-term responses to variability in nitrate inputs, and loads can be underestimated because rainfall event concentration peaks are absent (Buda and DeWalle, 2009; Meter et al., 2017; Outram et al., 2016).

The discharge-nitrate concentration relationship is complicated from the seasonal dynamics of nitrate transport. Spring runoff often carries the majority of annual nitrate load (Campbell et al., 2006; Brooks et al., 1998; Kincaid et al., 2020). Soil nitrate can accumulate during prolonged dry periods, which magnifies stream concentrations and loads when wet weather regimes return (Jones et al., 2016; Lucey and Goolsby, 1993). Fluctuations in seasonal and annual discharge-nitrate relationships have been examined, but often over monthly or annual time scales (Basu et al., 2012; Kelly et al., 2015; Schilling and Lutz, 2004; Van Meter and Basu, 2017). Increasingly, there have been advances in the use of in situ nutrient sensors that measure nitrate concentrations at higher, continuous temporal resolutions than previously used (Rode et al., 2016; Schwientek et al., 2013; Zimmer et al., 2019); however, these technologies can be costly to implement and do not yield a long-term perspective.

Stream nitrate concentrations and loads vary with different streamflow sources. Although surface runoff transports nitrate, many

studies have shown that it is mainly exported during baseflow conditions (Kang et al., 2008; Schilling and Lutz, 2004; Schilling and Zhang, 2004; Villarini et al., 2016). Nitrate's solubility allows it to infiltrate into the soil profile and shallow groundwater where it enters the stream network with baseflow (Kang et al., 2008). Loads have been shown to increase disproportionately with baseflow (Schilling and Zhang, 2004); furthermore, Schilling and Lutz (2004) found that nearly 2/3 of nitrate discharged to streams was through baseflow in an Iowa agricultural watershed. Other studies have found higher baseflow nitrate from agricultural landscapes compared with other land use types (i.e., forested and urban) (Vanni et al., 2001; Schilling and Zhang, 2004; Buda and DeWalle, 2009). Agricultural practices such as artificial drainage systems that quicken the delivery of precipitation to streams reduces the opportunity for nitrate to be retained and consumed by natural processes (Kincaid et al., 2020). For example, Tesoriero et al. (2009) reported that quickflow pathways (i.e., tile drains) were associated with higher concentrations than those found in streamflow (Hernández-García et al., 2020).

It can be difficult to disentangle the influence of different pathways because of the complexities associated with land use and discharge. Because Iowa agricultural watersheds have a large contribution to the Gulf of Mexico hypoxic zone, nitrate transport in Iowa has been studied extensively (e.g., Arenas Amado et al., 2017; Drake et al., 2018; Jones et al., 2018a, 2018b; Kelly et al., 2016; Schilling, 2005; Schilling and Lutz, 2004; Schilling and Wolter, 2001; Schilling and Zhang, 2004; Stenback et al., 2011; Villarini et al., 2016). Previous studies have examined how the components of streamflow influence nitrate, but their analyses have been limited in how they related nitrate with discharge, i.e. either using total streamflow, or examining stormflow and baseflow separately (e.g., Schilling and Lutz, 2004; Woodley et al., 2018). This paper aims to use the relationship between daily nitrate load and discharge to better understand hydrologic pathways and improve estimation of nitrate on days when monitoring data are absent. Specifically, we explore the relationship of streamflow and its two components (i.e., baseflow and stormflow) by comparing the results from four different models: one that only includes baseflow as a predictor, another using stormflow, a third model incorporating baseflow and stormflow, and a four model that uses streamflow (unseparated). This framework has the potential to estimate nitrate fluctuations on a finer scale than what has previously been reported.

2. Methods

2.1. Study area

Eight rivers across Iowa and their corresponding drainage areas were selected for this analysis (Fig. 1). The watersheds vary in size from 1020 to 4007 km². Three of the watersheds (Solider, East Nishnabotna and Floyd Rivers) drain to the Missouri River Basin, and five (Upper Iowa, English, Cedar Creek, North Raccoon, and North Rivers) drain to the Upper Mississippi River Basin. The watersheds lie within Iowa's different landform regions: Des Moines Lobe, Southern Iowa Drift Plane, Paleozoic Plateau and the Northwest Iowa Plains (Prior, 1991). The dominant land use in these watersheds is row crop farming of corn and soybeans (shown in Fig. 1 as the county level data

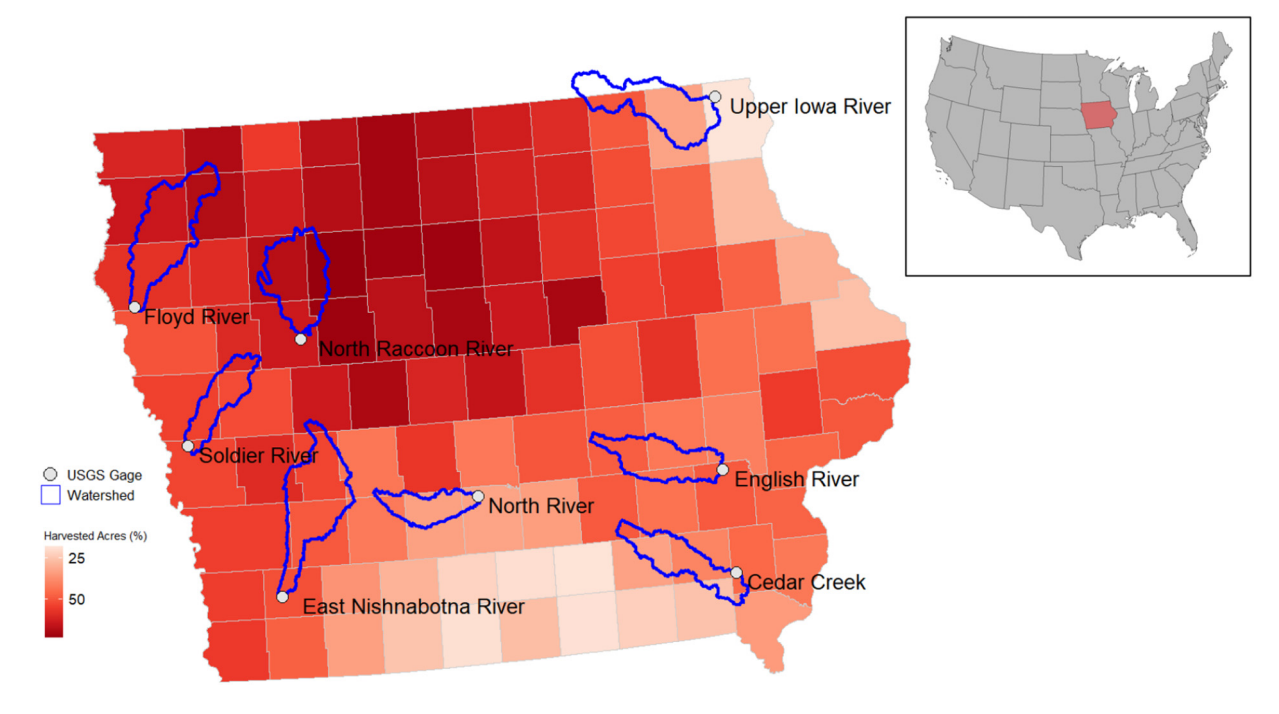


Fig. 1. Location of the eight United States Geological Survey (USGS) catchments in Iowa (corresponding to the Iowa Department of Natural Resources (IDNR) stations). Stream gauges are indicated as grey circles with their watershed boundaries (blue) which are overlaid on-top of the county level harvested acres of combined corn and soybeans in 2019. The figure in the top right corner shows the location of Iowa in the continental U.S.

reported as the fraction of total land dedicated to combined corn and soybean harvested acres in 2019). Harvested acres were reported as a fraction of the total land area dedicated to corn and soybeans, ranging from 0.43 to 0.81. See Table 1 for more details about the characteristics of each watershed analyzed in this study.

2.2. Data and statistical modeling

To assess the relationship between discharge and nitrate load, we evaluated the long-term water quality and discharge records at the outlets of the eight lowa watersheds shown in Fig. 1. The lowa Department of Natural Resources (IDNR) ambient monitoring program (IDNR, 2020) has been sampling each site monthly since 1987. Samples were generally taken during the first week of the month, but the exact date varies from month to month due to staffing and weather considerations. Starting from January 1987 and ending May 2019, the total number of observations among all eight watersheds ranged from 385 to 410 with a mean of 395. They are the longest continuous water quality monitoring records in the IDNR database. A US Environmental Protection Agency (USEPA) approved Quality Assurance Project Plan governed the program, and samples were analyzed by the State of lowa Hygienic

Laboratory using EPA Method 353.2 (O'Dell, 1996). The IDNR sites are co-located with U.S. Geological Survey (USGS) stream gauges, and daily average discharge data were downloaded from the USGS NWIS website (U.S. Geological Survey, 2016). Here we focus on the nitrate load reported as kg NO₃-N ha⁻¹ per day calculated by multiplying the concentration by daily mean discharge divided by watershed area. For each watershed, we calculated nitrate load only for the days that water quality samples were collected using all available water quality data over the record period (January 1987 to May 2019). We assume a negligible trend in nitrate load because row crop farming and nitrate concentrations have leveled off since the 1980s (i.e., over the time frame of this study period). Furthermore, Schilling and Zhang (2004) found no temporal trend in nitrate data or streamflow data over the 1972–2000 period for the Raccoon River in Iowa (at the 0.05 significance level).

Hydrograph separation was performed to analyze the relationship of load to baseflow and stormflow. To separate out baseflow from streamflow, digital filters can be applied over a continuous streamflow time series to obtain a time series of baseflow discharge. In this analysis, the one-parameter digital filter method by Lyne and Hollick (1979) was used because it has been shown to be an objective and reliable method

Table 1Watershed characteristic of the eight sites analyzed in this study. Column 2 reports the percentage of land dedicated to corn and soybeans (fraction of the total watershed area) as the mean over the last 11 years (2009–2019), Column 3 is the average annual precipitation (2002–2019), Column 4 is the average annual streamflow (1987–2019), and Column 5 refers to the Baseflow Index (BFI) for each watershed. The BFI is the long-term ratio of baseflow to total streamflow.

Station USGS station	Row Crop fraction	Average annual precipitation (2002–2019) mm	Average annual streamflow (1987–2019) m ³ /s	BFI
Upper Iowa River at Dorchester 05388250	0.43	921	7356	0.84
English River at Riverside 05455500	0.61	949	5047	0.82
Cedar Creek at Oakland Mills 05473400	0.45	956	4366	0.79
North Raccoon River at Sac City 05482300	0.81	790	4951	0.82
North River at Norwalk 05486000	0.55	943	2438	0.81
Floyd River at Sioux City 06600500	0.75	779	4185	0.84
Soldier River at Pisgah 06608500	0.72	842	2327	0.84
East Nishnabotna River at Shenandoah 06809500	0.70	870	7034	0.84

in the Midwest (Ayers et al., 2019; Nathan and McMahon, 1990; Xie et al., 2020). Baseflow is calculated using the following equation:

$$q_t = \alpha \times q_{t-1} + \frac{(1+\alpha)}{2} \times (Q_t - Q_{t-1}) \tag{1}$$

where q_t is the filtered runoff at the t time step; q_{t-1} is the filtered direct runoff at the t-1 time step; α is the a filter parameter or the recession constant; Q_t is the total streamflow at the t time step; and Q_{t-1} is the total streamflow at the t-1 time step. The recession constant represents the rate at which streamflow decreases after a rain event. We used $\alpha = 0.925$ because previous studies have found it to be a reliable value in the U.S. Midwest (Arnold and Allen, 1999; Ayers et al., 2020; Nathan and McMahon, 1990). To quantify the relative amount of annual baseflow in each watershed, we used the Baseflow Index (BFI) which measures baseflow as a fraction of total streamflow. The BFI was calculated over the 1980–2019 period (Table 1, column 4).

The objective of this study was to estimate nitrate load during nonanalyzed days using discharge data. IDNR grab samples are collected and reported as a daily point estimate, so each observation was related to the corresponding daily mean discharge. To predict nitrate load (dependent variable), we fit four statistical models using different independent variables, including one model that used daily baseflow discharge as a predictor, a second model using stormflow, a third model included baseflow and stormflow as predictors, and a fourth model using total streamflow. Total streamflow refers to streamflow discharge that is not separated into baseflow and stormflow components. Baseflow was estimated by applying the Lyne and Hollick one-parameter baseflow separation method to the streamflow time series. Stormflow was calculated as the difference between streamflow and baseflow. Before fitting the statistical models, we transformed the nitrate load and discharge time series. In R, the BoxCox.ar function in the Time Series Analysis (TSA) library determines an appropriate power transformation for a time-series dataset (Chan and Ripley, 2020). We found that the square root transformation was most appropriate for the nitrate load data since it applies to datasets with positive values and allows for a straightforward interpretation of the results. On the other hand, the logarithm transformation was used for the discharge data because it is a useful method for highly skewed data and produces a time series with approximately constant variance.

The Generalized Additive Model for Location Shape and Scale (GAMLSS; Stasinopoulos and Rigby, 2007) was used to develop the statistical models because it allows for a high degree of flexibility in terms of distributions and functional relationships in its parameters compared to other statistical models. We selected the dependence of the model's

parameters on covariates based on the Schwarz Bayesian Criterion (SBC; Schwarz, 1978) which generally results in a more parsimonious model than one obtained with respect to the Akaike Information Criterion (AIC; Akaike, 1978). The lognormal distribution was selected because it resulted in the best model fit between discharge and nitrate load compared with other distribution. A lognormal distribution is a good distribution for describing continuous variables that cannot take on negative values such as nitrate load. In these models, μ and σ are the two parameters of the lognormal distribution where μ was dependent on the discharge predictors in each model. We found that σ did not significantly depend on the covariates analyzed here, so it was held constant, with an estimated value that varied from site to site. Table 2 includes the model formulation and the parameters estimated for each model. Fig. 2 shows an example of the type of time series that was created for each of the eight sites (USGS site 05482300, North Raccoon River at Sac City, Iowa) see Figs. S1-S7 for time series of the other seven sites). We used the parameterization based on the GAMLSS package in R (Stasinopoulos and Rigby, 2007).

To quantify how well our models perform, we compute the Pearson's correlation coefficient, R, between the observations and the median of the fitted lognormal distribution (i.e., 50th quantile of the probabilistic model fit; Fig. 3 and Fig. S1-S7). Furthermore, we evaluate model performance based on the mean square error (MSE) skill score (SS_{MSE}) and its decomposition (Hashino et al., 2006):

$$SS_{MSE} = 1 - \frac{MSE}{\sigma_0^2} \tag{2}$$

where σ_0 is the standard deviation of the observations. A skill score of 1 indicates a perfect score, while lower values point to bias in the model predictions. A value of 0 is indicates that the performance of the model is the same as the climatology, while negative values point to a worse performance.

$$SS_{MSE} = \rho_{ro}^2 - \left[\rho_{ro} - \frac{\sigma_r}{\sigma_0}\right]^2 - \left[\frac{\mu_r - \mu_0}{\sigma_0}\right]^2 \tag{3}$$

where ρ_{ro}^2 is the potential skill (i.e., the skill if there were no biases) and ρ_{ro} represents the correlation coefficient. The $\left[\rho_{ro} - \frac{\sigma_r}{\sigma_0}\right]^2$ term calculates the conditional bias (i.e., the slope reliability (SREL)) where σ_r represents the standard deviation of the model predictions. The term $\left[\frac{\mu_r - \mu_0}{\sigma_0}\right]^2$ represents the unconditional bias (SME), where μ_r and μ_0 are the mean of the modeled and observational data, respectively. The decomposition of the skill score identifies conditional and unconditional bias in our model outputs.

Table 2Model formulations for each of the eight watersheds analyzed in this study. We model nitrate load (y_1) as a function of different discharge covariates. The observed discharge time series include the following: baseflow (x_b) , stormflow (x_q) , and total streamflow (x_t) . We used the square root transformation for nitrate load and the log transformation for all the discharge time series.

Station USGS station	Baseflow model formulation	Stormflow model formulation	Baseflow-stormflow model formulation	Streamflow model formulation
Upper Iowa River at Dorchester	$sqrt(y_1) = -3.56 + 0.76$	$sqrt(y_1) = -2.0 + 0.30$	$sqrt(y_1) = -3.18 + 0.52 \cdot \log(x_b) + 0.17$	$sqrt(y_1) = -3.70 + 0.71$.
05388250	$\log(x_b)$	$\log(x_q)$	$\cdot \log(x_q)$	$\log(x_t)$
English River at Riverside	$sqrt(y_1) = -2.92 + 0.74$.	$sqrt(y_1) = -2.23 + 0.40$	$sqrt(y_1) = -2.68 + 0.39 \cdot \log(x_b) + 0.26$	$sqrt(y_1) = -3.72 + 0.82$.
05455500	$\log(x_b)$	$\log(x_q)$	$\cdot \log(x_q)$	$\log(x_t)$
Cedar Creek at Oakland Mills	$sqrt(y_1) = -2.67 + 0.71$.	$sqrt(y_1) = -2.32 + 0.41$	$sqrt(y_1) = -2.56 + 0.36 \cdot \log(x_b) + 0.22$	$sqrt(y_1) = -3.6 + 0.80$.
05473400	$\log(x_b)$	$\log(x_q)$	$\cdot \log(x_q)$	$\log(x_t)$
North Raccoon River at Sac City	$sqrt(y_1) = -2.46 + 0.60$.	$sqrt(y_1) = -1.97 + 0.37$	$sqrt(y_1) = -2.40 + 0.38 \cdot \log(x_b) + 0.22$	$sqrt(y_1) = -2.75 + 0.53$.
05482300	$og(x_b)$	$\log(x_q)$	$\cdot \log(x_q)$	$\log(x_t)$
North River at Norwalk	$sqrt(y_1) = -2.44 + 0.60$.	$sqrt(y_1) = -2.13 + 0.40$	$sqrt(y_1) = -2.37 + 0.38 \cdot \log(x_b) + 0.21$	$sqrt(y_1) = -3.16 + 0.73$.
05486000	$\log(x_b)$	$\log(x_q)$	$\cdot \log(x_q)$	$\log(x_t)$
Floyd River at Sioux City	$sqrt(y_1) = -2.92 + 0.70$.	$sqrt(y_1) = -1.94 + 0.35$.	$sqrt(y_1) = -2.79 + 0.54 \cdot \log(x_b) + 0.18$	$sqrt(y_1) = -3.20 + 0.68$.
06600500	$\log(x_b)$	$\log(x_q)$	$\cdot \log(x_q)$	$\log(x_t)$
Soldier River at Pisgah	$sqrt(y_1) = -2.80 + 0.71$.	$sqrt(y_1) = -1.87 + 0.25$.	$sqrt(y_1) = -2.67 + 0.61 \cdot \log(x_b) + 0.12$	$sqrt(y_1) = -3.02 + 0.70$.
06608500	$\log(x_b)$	$\log(x_q)$	$\cdot \log (x_q)$	$\log(x_t)$
East Nishnabotna River at Shenandoah	$sqrt(y_1) = -3.27 + 0.67$.	$sqrt(y_1) = -2.21 + 0.34$	$sqrt(y_1) = -3.15 + 0.50 \cdot \log(x_b) + 0.20$	$sqrt(y_1) = -3.92 + 0.76$.
06809500	$\log(x_b)$	$\log(x_q)$	$\cdot \log(x_q)$	$\log(x_t)$

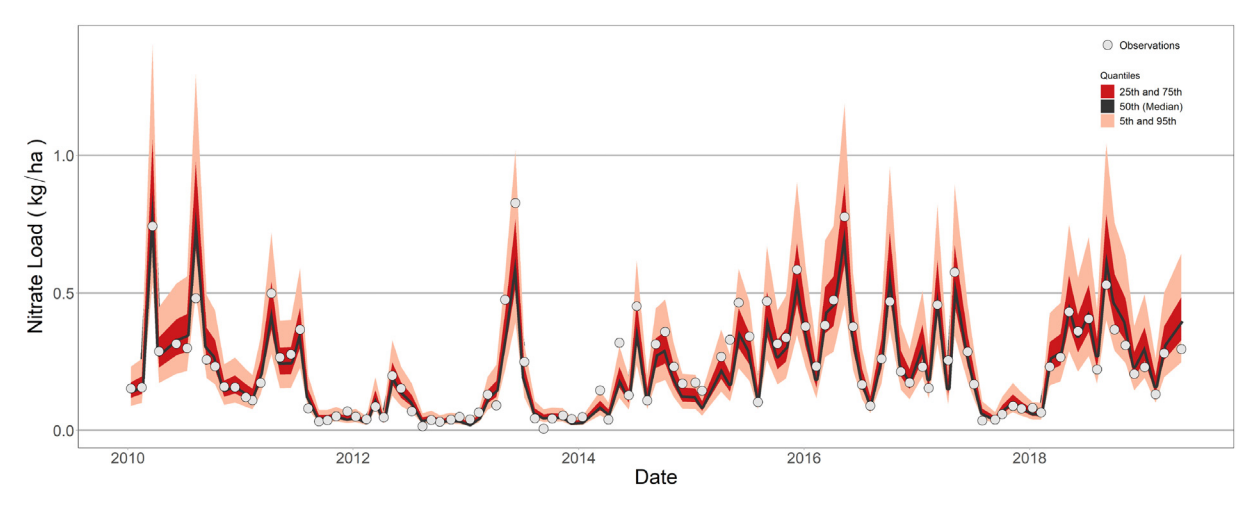


Fig. 2. An example of the type of time series that was created for each of the eight sites illustrating the probabilistic model fit (USGS site 05482300; North Raccoon River at Sac City, Iowa). Here, we illustrate the model fit over the last 10 years (2010–2019) for simplicity and visualization of model fit. The median is shown as a black line, while the area between the 5th and 95th (25th and 75th) percentiles are shaded in red (lighter red). The monthly observations are shown as grey points for comparison. Time series for all sites over the entire record (1987–2019) are reported in Figs. S1-S7.

3. Results

To estimate daily nitrate load, we modeled load as a function of daily discharge using observations over the study period (1987 to 2019). The results from four different model formulations were analyzed: one had baseflow as a covariate, one had stormflow, and a third model included both baseflow and stormflow as covariates, and a fourth model using total streamflow. As an example of how well the baseflow-stormflow models reproduced observational records, Fig. 2 shows the time series (from 2010 to 2019) of the probabilistic model fit for the North Raccoon

River at Sac City, Iowa. Although the results in Fig. 2 reference a single site, model and shorted time frame, the same plots for all sites and models were produced over the entire record period (Supplemental material S1-S7 using the baseflow-stormflow model; the figures for the baseflow and stormflow models are omitted for simplicity).

To compare between models, the Pearson's correlation coefficient and skill score were calculated between the grab sample observations and the median (50th quantile) of the probabilistic model fits (Figs. 3 and 4). Overall, the baseflow-stormflow models performed the best by both methods. The mean of correlation coefficients (skill scores) across

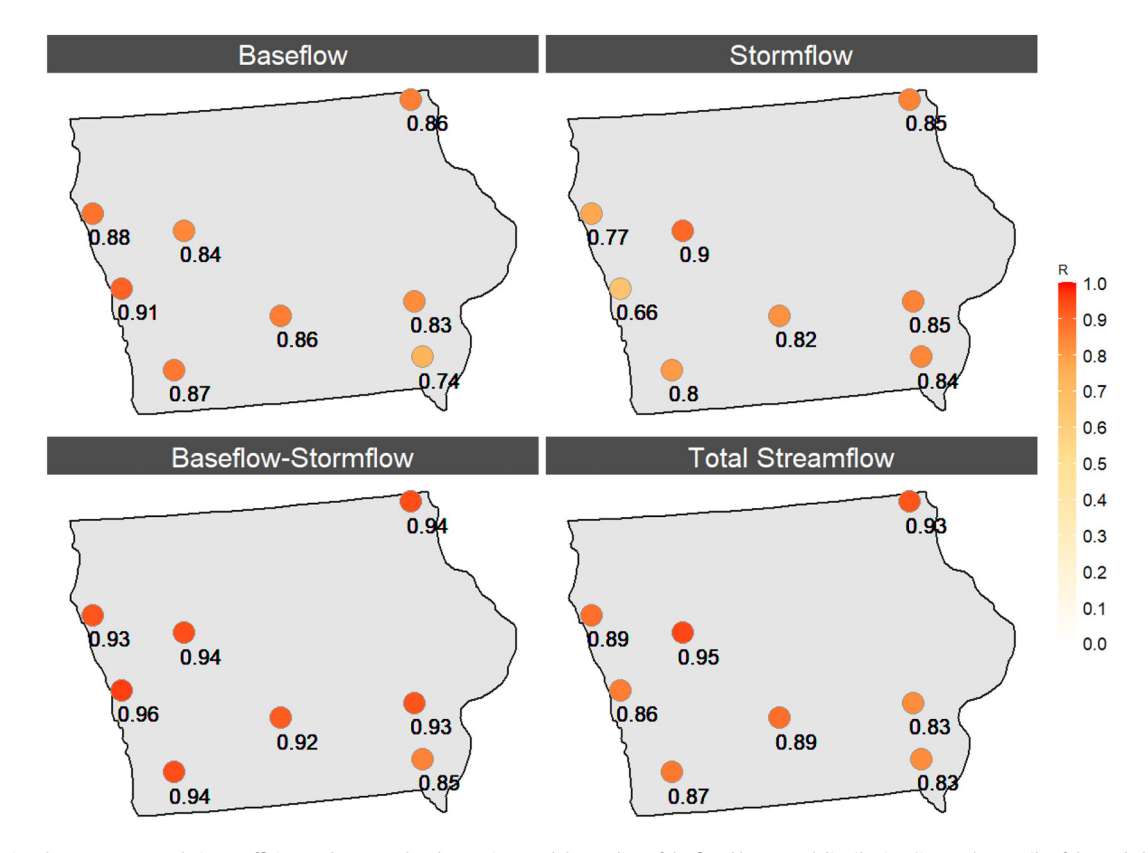


Fig. 3. Map showing the Pearson's correlation coefficient, R, between the observations and the median of the fitted lognormal distribution (i.e., 50th quantile of the probabilistic model fit) at each station. The four different model results are reported (baseflow, stormflow, baseflow-stormflow, and total streamflow).

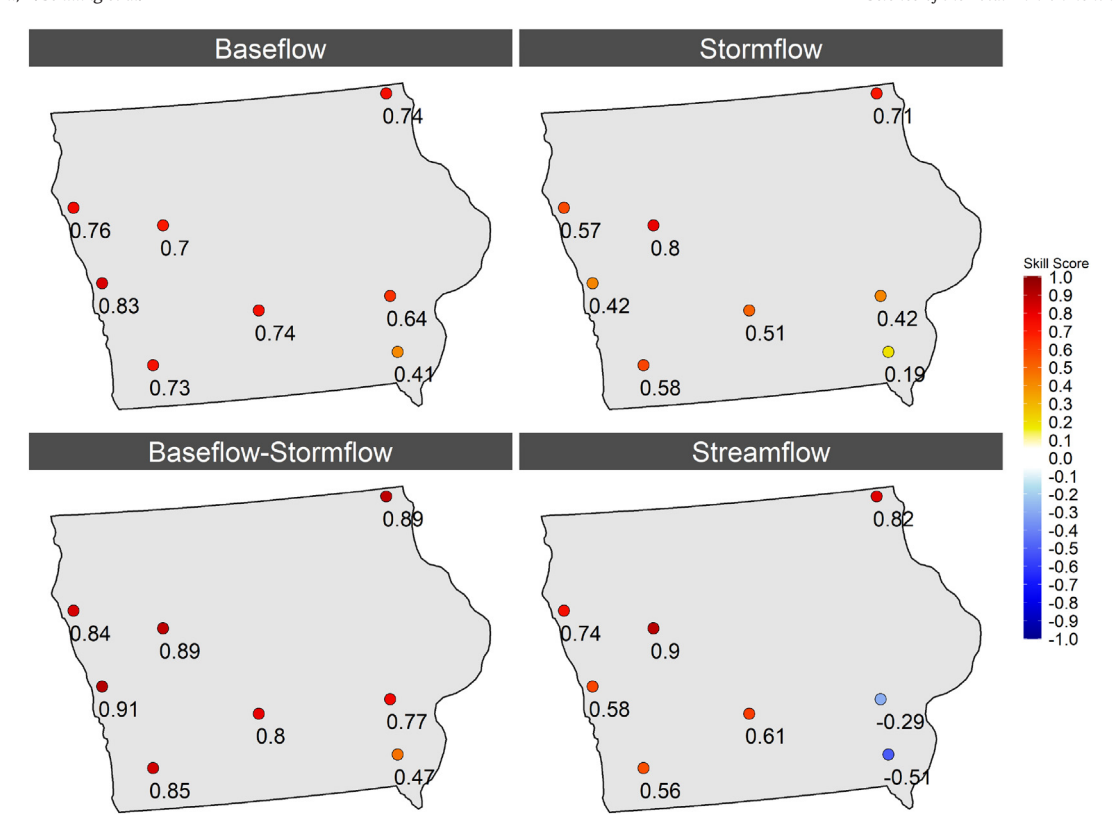


Fig. 4. Maps illustrating the skill score between the daily grab samples and the median of the model fit (i.e., 50th quantile of the probabilistic model fit) at each station, highlighting the limited impacts of conditional and unconditional biases. The results include the baseflow, stormflow, baseflow-stormflow, and total streamflow models.

all sites and for each model included: 0.92 (0.80) for the stormflowbaseflow models, 0.85 (0.69) with respect to the baseflow models, 0.81 (0.52) for the stormflow models, and 0.88 (0.42) for the streamflow models. These results highlight variability among the performance of each model. While the streamflow models performed second best (on average) by the correlation coefficient, the skill scores indicated bias in these models, particularly in southeast Iowa where negative skill scores were reported. The skill score is more sensitive to extreme values, and the streamflow models tended to overestimate large nitrate loads compared with observations. On the other hand, the baseflow and baseflow-stormflow models were more skillful, likely because their peak load values were not as extreme, and baseflow accounts for a large portion of nitrate loads. In other words, because baseflow is modeled separately, the baseflow-stormflow and baseflow models predicted nitrate loads better during the entire year, especially from September to February when peak loads are negligible.

Furthermore, the scatterplots in Fig. 5 illustrate how well each model fit by comparing the observations to the corresponding predicted median value (50th quantile of the probabilistic model fit) for all sites. The baseflow-stormflow models showed the best agreement with the observations (Fig. 5, column 3). Daily predicted values followed the one-to-one line tightly, giving evidence of the models' ability to capture nitrate loads. The difference between the baseflow-stormflow and total streamflow models illustrated that the baseflow-stormflow models capture higher nitrate loads better (Fig. 5 columns 3 and 4). The baseflow-stormflow models had the highest correlation coefficients, followed by the streamflow models, but model performance varied between the baseflow models and the stormflow models. Baseflow was a better predictor at lower nitrate loads (Fig. 5, first column). Overall, predictions from this model matched observations well, but the baseflow models had a tendency to underestimate larger nitrate loads. Higher nitrate loads are associated with stormflow as precipitation events mobilize copious amounts of nitrate held within the soil profile. As a result, the stormflow models better captured nitrate loads in the upper part of the distribution; however, the stormflow models had more difficulty estimating lower loads (Fig. 5, column 3). The baseflow-stormflow models borrow strength from both components of streamflow, estimating values more accurately across the entire nitrate load distribution.

To obtain load estimates for non-analyzed days, daily discharge data were used as inputs in the model formulations. Fig. 6 shows the type of time series created using the median (i.e., 50th quantile) predicted value from each model fit for the North Raccoon River at Sac City (March 2017 to August 2018; see Supplemental Materials S8-S14 for a daily time series at every station). It is important to note that the grab sample observations are only available at a frequency of one per month (grey circles), while the models produce daily estimates. Here, we observed clear differences in how each model estimates daily nitrate loads. The baseflow models estimated steadier changes in loads from day to day compared to the other three models. By only using baseflow as a predictor, the model did not increase drastically nor did it capture the variability associated with peak loads. The stormflow models estimated larger nitrate loads, but the peaks were more extreme compared with the baseflow and baseflow-stormflow models. Daily estimates using the baseflow-stormflow model lied between the baseflow and stormflow models. On the other hand, streamflow model estimates for peak loads were drastically larger than any other model. Because these models treat baseflow and streamflow the same, it is likely that they cannot capture differences in loads exported through two separate processes. Since the baseflow-stormflow models incorporate the bulk of nitrate load from baseflow with the addition of nitrate mobilized with stormflow, they captured loads during baseflow conditions as well as the increased variability associated with stormflow.

4. Discussion

The results reported here highlight key differences in the nitratedischarge relationship. Although the baseflow-stormflow and streamflow

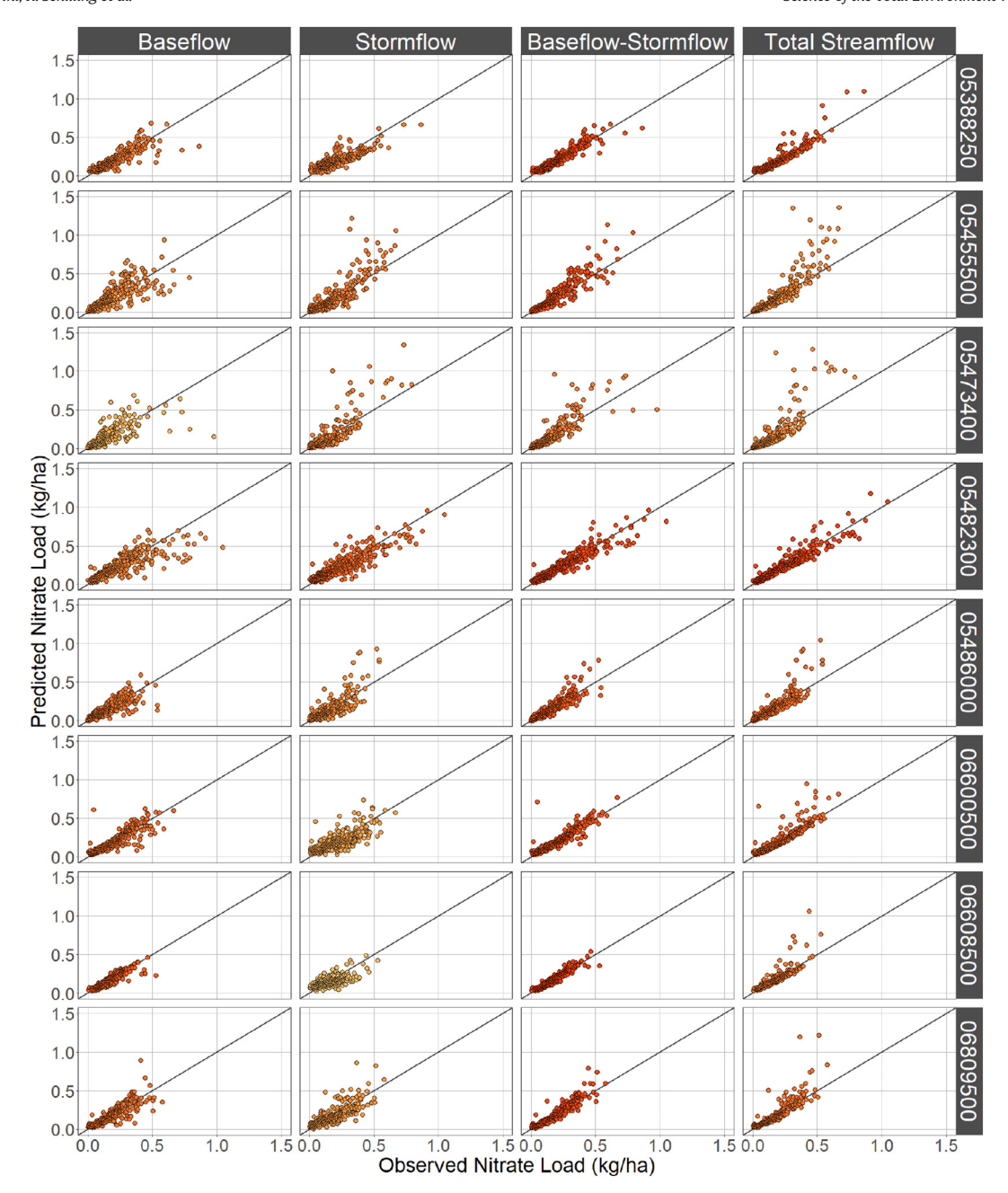


Fig. 5. Scatterplots comparing the relationship between the observational record and the median of the daily model predictions (50th quantile of the probabilistic model fit). Each column corresponds to the different models and the rows indicate the station results. The fill color represents the correlation coefficient over the entire record (1987–2019), as reported in Fig. 3.

models performed well overall ($R \ge 0.83$), the baseflow-stormflow models performed the best, which highlights the importance of separating out the components of streamflow. The distinction between baseflow and stormflow is critical from March to August when stormflow loads are associated with seasonal precipitation. From September to February, the models are nearly identical because streamflow consists almost entirely of baseflow and nitrate loads are substantially smaller. Thus, baseflow is a more important predictor during low-flow months and in watersheds that have a larger baseflow contribution. It is interesting to note that in some watersheds the correlation coefficient was higher for the baseflow model, whereas in others stormflow was a better predictor. Among the eight rivers, the differences in model performance can be attributed to differences in land use, watershed characteristics, and climate. In this study, we only speculate on watershed characteristics because Jones et al.

(2018a, 2018b) already examined the impact of precipitation for these watersheds. Rather, we contextualize our modeling results by analyzing how topography, geology and land use could control surface and subsurface pathways.

The Floyd River, Soldier River and East Nishnabotna River have baseflow models that performed better than the stormflow models. These watersheds are located in western Iowa and drain to the Missouri River, in contrast to the other five catchments which drain to the Upper Mississippi River. The geology of the Floyd River, Solider River and East Nishnabotna River is characterized by thick deposits of wind-blown loess capping fine-textured glacial till (Jones et al., 2018b; Prior, 1991). These watersheds characteristics could be responsible for more streamflow being routed through baseflow, which would drive the relationship between baseflow and nitrate load. Other studies conducted in

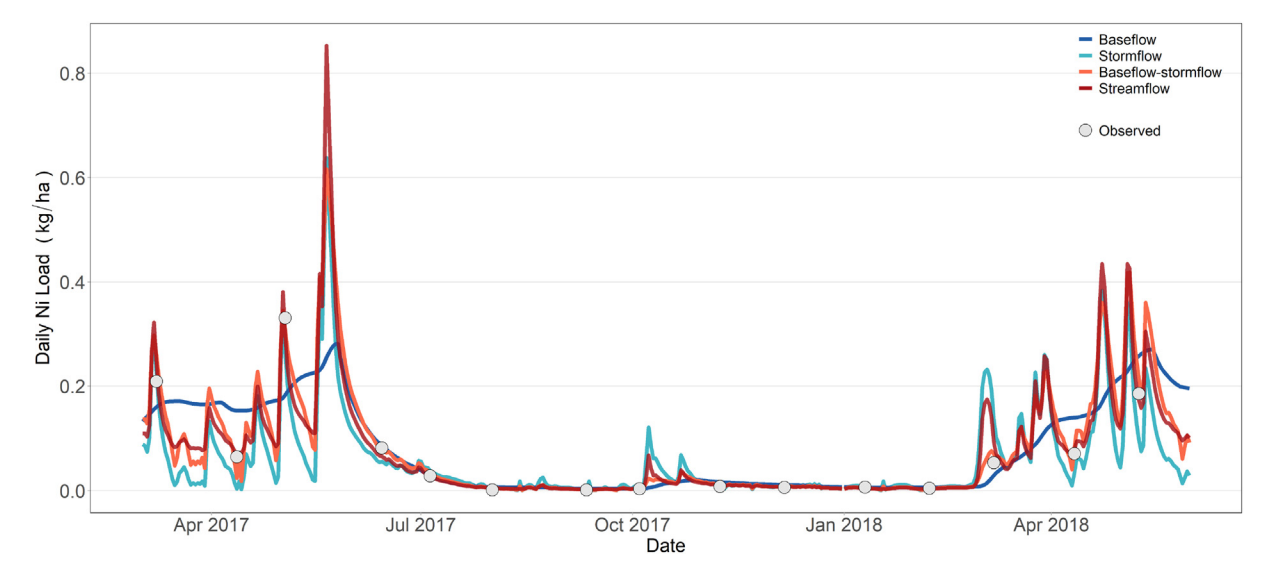


Fig. 6. Daily nitrate load predictions based on models in which baseflow is the only predictor (red line), stormflow is the only covariate (blue line), one in which both quantities are used as predictors (green line), and one model that uses total streamflow as a predictor (grey line). The grey points are the monthly grab sample observations reported as the calculated daily nitrate load. As an example, this time series shows the estimated daily values from March 2017 to August 2018 for the North Raccoon River at Sac City.

lowa found that baseflow contributes to nitrate loads more than stormflow (Richards et al., 2021; Schilling and Lutz, 2004; Schilling and Zhang, 2004). For example, Schilling and Zhang (2004) proposed the term "baseflow enrichment ratio (BER)" to describe how baseflow was enriched with greater nitrate load relative to the baseflow water flux alone. Both the current study and Schilling and Zhang (2004) show the importance of baseflow in contributing to nitrate loads in agricultural watersheds in Iowa.

On the other hand, the stormflow models in the Upper Iowa, English River, Cedar Creek, North Raccoon and North River outperformed the baseflow models. Geology, topography, and land use and land management practices can alter nitrate inputs and transport pathways (Kincaid et al., 2020; Villarini et al., 2016), and these drivers could be at work here. The Upper Iowa River watershed is dominated by steep slopes underlain by fractured and karstic shallow bedrock that feeds local rivers with groundwater baseflow and springs (Jones et al., 2018b; Prior, 1991), whereas the landscape draining to the southern Iowa watersheds of the English River, North River, and Cedar Creek consists of rolling hills of thin loess over glacial till that produce more stormflow (Schilling and Libra, 2003). The topography in all of these watersheds is dominated by hillslopes which is consistent with stormflow contributions to nitrate loads. Contrastingly, the North Raccoon River watershed is one with low relief and extensive tile drainage and we would not have suspected major stormflow correlation to nitrate loads (Jones et al., 2016). However, in extensively tile-drained watersheds like the North Raccoon, the tile network can behave like a subsurface "karst" system delivering stormflow loads to streams (Schilling and Helmers, 2008). Furthermore, in the Cedar Creek watershed the performance of the stormflow model (R value = 0.84) was similar to the baseflowstormflow model (0.85), and the baseflow model performed worse (0.74) than at any other site. In this watershed, the BFI is slightly lower relative to the seven other watersheds (Table 1, column 4). A lower BFI could indicate that more streamflow is sourced from stormflow, carrying a higher proportion of nitrate with it. It should be considered that these hydrological differences may be lessened or masked by Iowa's crop production system. Annual crops of corn and soybeans are dominant in all watersheds, with similar planting and harvesting times, input amounts, and production methods. Only the Upper Iowa watershed is distinctly different from a crop production standpoint because of its lower fraction of row crop area. A diversity of hydrological drivers of nitrate transport may be present and variable among watersheds, but because the crop production system itself may be the largest hydrological driver, the others do not produce a strong enough nitrate signal to be apparent.

These results further highlight the seasonality of the dischargenitrate relationship, along with stormflow's influence on nitrate load variability. Models were more skillful at predicting nitrate load during baseflow conditions (September to February), but there were discrepancies between peak loads and model fit. Daily average stormflow may not be fine enough to capture the nitrate discharged with individual precipitation events, particularly during strong summertime storms. To determine the magnitude of stormflow loads, we would either need grab sample observations during large precipitation events or a dataset with a shorter time step; however, data are difficult to obtain and/or not available on a long-term scale (Arenas Amado et al., 2017; Duncan et al., 2017; Miller et al., 2017; Schwientek et al., 2013). Although the utility of this methodology is that it uses readily available discharge data to estimate daily nitrate loads, there is still some variability left unexplained. There is a potential for other varying hydrologic conditions to improve estimates, such as antecedent wetness, precipitation events (magnitude and intensity), and seasonal influence. These models could also be improved by including additional predictors such as fertilizer application data and land use types. In agricultural watersheds, higher nitrate concentrations are associated with fertilizer application during the growing season (March to August). Thus, including this information could improve our models; however, fertilizer application datasets are not readily available and are difficult to implement in practice because nitrate delivered to streams also depends on plant uptake of nitrate (Yue et al., 2019).

Predicting nitrate loads during baseflow and stormflow conditions has important implications for effective nutrient management practices. Despite their simplicity, these regression models can be used to understand nitrate loads delivered through surface and subsurface processes. They can be used to identify when a pathway is likely to have large loads, and target nutrient reduction practices accordingly. In particular, these results show that methods that estimate nitrate loads with total streamflow could be over estimating nitrate exports during extreme events. Our model estimates of daily loads may track more accurately with nitrate delivered to streams, providing an alternative way to calculate annual loads. Albeit simple, this modeling framework can be

applied in other watersheds with similar water quality issues. More research is needed to understand nitrate behavior and its controls during peak run-off events.

5. Conclusions

In this study we compared three different model formulations to understand the relationship of daily nitrate load with different components of the hydrograph. The model formulations included: one using baseflow as a predictor, another with stormflow, a third mode that included both baseflow and stormflow, and a final model using total streamflow. Each model's performance was evaluated by calculating the correlation coefficient between the observational record and the median of the model fit. Overall, the baseflow-stormflow models yielded the best model fit for all sites. These results highlight the importance of modeling baseflow and stormflow separately because of the differences in their relative contributions throughout the year. While baseflow was a better predictor at lower loads, stormflow captured larger nitrate loads and the variability associated with peak events. Between the baseflow models and stormflow models, there were differences in model performance across the eight watersheds. For catchments located in the western part of Iowa, where thick loess soils predominate (Soldier River, Floyd River and East Nishnabotna River), the baseflow model performed better than the stormflow model, indicating that baseflow water yield may be contributing more to nitrate load. On the other hand, stormflow models in the Upper Iowa, North Raccoon, North, English and Cedar Creek basins showed similar or slightly improved correlation with observational records than the models that used baseflow alone. In these watersheds thinner topsoils, subsurface drainage, and Karst topography may be distinguishing. The differences in geologic and tile drainage characteristics contribute to the variability in nitrate loads, and is dominated by stormflow in these watersheds more than in those western Iowa. The framework developed here could be improved by considering other predictors or using higher frequency water quality data to validate models. More work is needed to resolve the relative contribution of baseflow and stormflow to nitrate load.

CRediT authorship contribution statement

Jessica R. Ayers: Conceptualization, Formal analysis, Methodology, Software, Writing – original draft. Gabriele Villarini: Conceptualization, Methodology, Writing – review & editing, Funding acquisition. Keith Schilling: Conceptualization, Validation, Writing – review & editing. Christopher Jones: Conceptualization, Validation, Writing – review & editing.

Declaration of competing interest

The authors declare that they have no known competing financial interests or personal relationships that could have appeared to influence the work reported in this paper.

Acknowledgments

This study was supported in part by the National Science Foundation under grant number DGE 1633098, and by Iowa State University under Iowa Development Authority Award No. 13-NDRP-016 through funding from the U.S. Department of Housing and Urban Development. The suggestions by seven anonymous reviewers are gratefully acknowledged.

Appendix A. Supplementary data

Supplementary data to this article can be found online at https://doi.org/10.1016/j.scitotenv.2021.146643.

References

- Akaike, H., 1978. On the likelihood of a time series model. Journal of the Royal Statistical Society. Series D (The Statistician) 27, 217–235.
- Arenas Amado, A., Schilling, K.E., Jones, C.S., Thomas, N., Weber, L.J., 2017. Estimation of tile drainage contribution to streamflow and nutrient loads at the watershed scale based on continuously monitored data. Environ. Monit. Assess. 189, 426.
- Arnold, J.G., Allen, P.M., 1999. Automated methods for estimating baseflow and ground water recharge from streamflow records 1. JAWRA Journal of the American Water Resources Association 35, 411–424.
- Ayers, J.R., Villarini, G., Jones, C., Schilling, K., 2019. Changes in monthly baseflow across the U.S. Midwest. Hydrol. Process. 33, 748–758.
- Ayers, J.R., Villarini, G., Schilling, K., and Jones, C. (2020). On the statistical attribution of changes in monthly baseflow across the U.S. Midwest. Journal of hydrology 125551.
- Basu, N.B., Jindal, P., Schilling, K.E., Wolter, C.F., Takle, E.S., 2012. Evaluation of analytical and numerical approaches for the estimation of groundwater travel time distribution. J. Hydrol. 475, 65–73.
- Brooks, P.D., Williams, M.W., Schmidt, S.K., 1998. Inorganic nitrogen and microbial biomass dynamics before and during spring snowmelt. Biogeochemistry 43, 1–15.
- Buda, A.R., DeWalle, D.R., 2009. Dynamics of stream nitrate sources and flow pathways during stormflows on urban, forest and agricultural watersheds in central Pennsylvania, USA. Hydrol. Process. 23, 3292–3305.
- Campbell, J.L., Mitchell, M.J., Mayer, B., 2006. Isotopic assessment of NO3— and SO42— mobility during winter in two adjacent watersheds in the Adirondack Mountains. New York. Journal of Geophysical Research: Biogeosciences 111.
- Chan, K.-S., Ripley, B., 2020. TSA: Time Series Analysis.
- Drake, C.W., Jones, C.S., Schilling, K.E., Amado, A.A., Weber, L.J., 2018. Estimating nitratenitrogen retention in a large constructed wetland using high-frequency, continuous monitoring and hydrologic modeling. Ecol. Eng. 117, 69–83.
- Duncan, J.M., Welty, C., Kemper, J.T., Groffman, P.M., Band, L.E., 2017. Dynamics of nitrate concentration-discharge patterns in an urban watershed. Water Resour. Res. 53, 7349–7365
- Goolsby, D.A., Battaglin, W.A., Aulenbach, B.T., Hooper, R.P., 2000. Nitrogen flux and sources in the Mississippi River Basin. Sci. Total Environ. 248, 75–86.
- Guo, Y., Markus, M., and Demissie, M. (2002). Uncertainty of nitrate-N load computations for agricultural watersheds. Water Resources Research 38, 3-1-3-12.
- Hansen, J.R., Refsgaard, J.C., Hansen, S., Ernstsen, V., 2007. Problems with heterogeneity in physically based agricultural catchment models. J. Hydrol. 342, 1–16.
- Hashino, T., Bradley, A.A., Schwartz, S.S., 2006. Evaluation of bias-correction methods for ensemble streamflow volume forecasts. Hydrol. Earth Syst. Sci. Discuss. 3, 561–594.
- Hernández-García, I., Merchán, D., Aranguren, I., Casalí, J., Giménez, R., Campo-Bescós, M.A., Del Valle de Lersundi, J., 2020. Assessment of the main factors affecting the dynamics of nutrients in two rainfed cereal watersheds. Sci. Total Environ. 733, 139177.
- Husic, A., Fox, J., Adams, E., Ford, W., Agouridis, C., Currens, J., Backus, J., 2019. Nitrate pathways, processes, and timing in an agricultural karst system: development and application of a numerical model. Water Resour. Res. 55, 2079–2103.
- IDNR, 2020. Iowa's Ambient Water Quality Monitoring and Assessment Program.
- Jones, C.S., Seeman, A., Kyveryga, P.M., Schilling, K.E., Kiel, A., Chan, K.-S., Wolter, C.F., 2016. Crop rotation and Raccoon River nitrate. J. Soil Water Conserv. 71, 206–219.
- Jones, C.S., Nielsen, J.K., Schilling, K.E., Weber, L.J., 2018a. Iowa stream nitrate and the Gulf of Mexico. PLoS One 13, e0195930.
- Jones, C.S., Schilling, K.E., Simpson, I.M., Wolter, C.F., 2018b. Iowa stream nitrate, discharge and precipitation: 30-year perspective. Environ. Manag. 62, 709–720.
- Kang, S., Lin, H., Gburek, W.J., Folmar, G.J., Lowery, B., 2008. Baseflow nitrate in relation to stream order and agricultural land use. J. Environ. Qual. 37, 808–816.
- Kelly, S.A., Takbiri, Z., Belmont, P., and Foufoula-Georgiou, E. (2016). Human amplified changes in precipitation-runoff patterns in large river basins of the Midwestern United States. Hydrology and Earth System Sciences Discussions 1–43.
- Kelly, V., Stets, E.G., Crawford, C., 2015. Long-term changes in nitrate conditions over the 20th century in two Midwestern Corn Belt streams. J. Hydrol. 525, 559–571.
- Kincaid, D.W., Seybold, E.C., Adair, E.C., Bowden, W.B., Perdrial, J.N., Vaughan, M.C.H., and Schroth, A.W., 2020 Land use and season influence event-scale nitrate and soluble reactive phosphorus exports and export stoichiometry from headwater catchments. Water Resources Research n/a, e2020WR027361.
- Lee, C.J., Hirsch, R.M., Schwarz, G.E., Holtschlag, D.J., Preston, S.D., Crawford, C.G., Vecchia, A.V., 2016. An evaluation of methods for estimating decadal stream loads. J. Hydrol. 542, 185–203.
- Lucey, K.J., Goolsby, D.A., 1993. Effects of climatic variations over 11 years on nitratenitrogen concentrations in the Raccoon River, Iowa. J. Environ. Qual. 22, 38–46.
- Lyne, V., and Hollick, M. (1979). Stochastic time-variable rainfall-runoff modeling. P. Meter, K.J.V., Basu, N.B., Cappellen, P.V., 2017. Two centuries of nitrogen dynamics: legacy
- Meter, K.J.V., Basu, N.B., Cappellen, P.V., 2017. Two centuries of nitrogen dynamics: legacy sources and sinks in the Mississippi and Susquehanna River Basins. Glob. Biogeochem. Cycles 31, 2–23.
- Miller, M.P., Tesoriero, A.J., Hood, K., Terziotti, S., Wolock, D.M., 2017. Estimating discharge and nonpoint source nitrate loading to streams from three end-member pathways using high-frequency water quality data. Water Resour. Res. 53, 10201–10216.
- Nathan, R.J., McMahon, T.A., 1990. Evaluation of automated techniques for base flow and recession analyses. Water Resour. Res. 26, 1465–1473.
- Nikolaidis, N.P., Bouraoui, F., Bidoglio, G., 2013. Hydrologic and geochemical modeling of a karstic Mediterranean watershed. J. Hydrol. 477, 129–138.
- O'Dell, J.W. (1996). Determination of nitrate-nitrite nitrogen by automated colorimetry. In Methods for the Determination of Metals in Environmental Samples, (Elsevier), pp. 464–478.
- Outram, F.N., Cooper, R.J., Sünnenberg, G., Hiscock, K.M., Lovett, A.A., 2016. Antecedent conditions, hydrological connectivity and anthropogenic inputs: factors affecting

- nitrate and phosphorus transfers to agricultural headwater streams. Sci. Total Environ. 545-546, 184-199.
- Prior, J., 1991. Landforms of Iowa. University of Iowa Press, Iowa City, IA.
- Richards, G., Gilmore, T.E., Mittelstet, A.R., Messer, T.L., Snow, D.D., 2021, Baseflow nitrate dynamics within nested watersheds of an agricultural stream in Nebraska, USA. Agric. Ecosyst, Environ, 308, 107223.
- Rode, M., Wade, A.J., Cohen, M.J., Hensley, R.T., Bowes, M.J., Kirchner, J.W., Arhonditsis, G.B., Jordan, P., Kronvang, B., Halliday, S.J., et al., 2016. Sensors in the stream: the high-frequency wave of the present. Environ. Sci. Technol. 50, 10297-10307
- Schilling, K., Zhang, Y.-K., 2004. Baseflow contribution to nitrate-nitrogen export from a large, agricultural watershed, USA. J. Hydrol. 295, 305-316.
- Schilling, K.E., 2005. Relation of baseflow to row crop intensity in Iowa. Agric. Ecosyst. Environ, 105, 433-438.
- Schilling, K.E., Helmers, M., 2008. Effects of subsurface drainage tiles on streamflow in Iowa agricultural watersheds: exploratory hydrograph analysis. Hydrol. Process. 22, 4497-4506
- Schilling, K.E., Libra, R.D., 2003. Increased baseflow in Iowa over the second half of the 20th Century1. JAWRA Journal of the American Water Resources Association 39, 851-860
- Schilling, K.E., Lutz, D.S., 2004. Relation of nitrate concentrations to baseflow in the Raccoon River, Iowa1. JAWRA Journal of the American Water Resources Association 40, 289_900
- Schilling, K.E., Thompson, C.A., 2000. Walnut Creek watershed monitoring project, Iowa monitoring water quality in response to prairie restoration1. JAWRA Journal of the American Water Resources Association 36, 1101-1114.
- Schilling, K.E., Wolter, C.F., 2001. Contribution of base flow to nonpoint source pollution loads in an agricultural watershed. Groundwater 39, 49-58.
- Schilling, K.E., Jones, C.S., Wolter, C.F., Liang, X., Zhang, Y.-K., Seeman, A., Isenhart, T., Schnoebelen, D., Skopec, M., 2017. Variability of nitrate-nitrogen load estimation results will make quantifying load reduction strategies difficult in Iowa. J. Soil Water Conserv. 72, 317-325.
- Schubert, S.D., Suarez, M.J., Pegion, P.J., Koster, R.D., Bacmeister, J.T., 2004. Causes of longterm drought in the U.S. Great Plains. J. Climate 17, 485-503.
- Schwarz, G., 1978. Estimating the dimension of a model. Ann. Stat. 6, 461-464.
- Schwientek, M., Osenbrück, K., Fleischer, M., 2013. Investigating hydrological drivers of nitrate export dynamics in two agricultural catchments in Germany using highfrequency data series. Environ. Earth Sci. 69, 381-393.

- Stasinopoulos, D.M., and Rigby, R.A. (2007), Generalized Additive Models for Location Scale and Shape (GAMLSS) in R. Journal of Statistical Software 23.
- Stenback, G.A., Crumpton, W.G., Schilling, K.E., Helmers, M.J., 2011. Rating curve estimation of nutrient loads in Iowa rivers. J. Hydrol. 396, 158–169.
- Tesoriero, A.J., Duff, J.H., Wolock, D.M., Spahr, N.E., Almendinger, J.E., 2009. Identifying pathways and processes affecting nitrate and orthophosphate inputs to streams in agricultural watersheds. J. Environ. Qual. 38, 1892–1900.
- U.S. Geological Survey (2016). USGS water data for the Nation; U.S. Geological Survey National Water Information System database.
- US EPA, O. (2015). Environmental Radiation Protection Standards for Nuclear Power Operations (40 CFR Part 190)
- Van Meter, K.J., Basu, N.B., 2017. Time lags in watershed-scale nutrient transport: an exploration of dominant controls. Environ. Res. Lett. 12, 084017.
- Vanni, M.J., Renwick, W.H., Headworth, J.L., Auch, J.D., Schaus, M.H., 2001. Dissolved and particulate nutrient flux from three adjacent agricultural watersheds: a five-year study, Biogeochemistry 54, 85-114.
- Villarini, G., Jones, C.S., Schilling, K.E., 2016. Soybean area and baseflow driving nitrate in Iowa's Raccoon River. J. Environ. Qual. 45, 1949-1959.
- Wherry, S.A., Tesoriero, A.J., Terziotti, S., 2021. Factors affecting nitrate concentrations in stream base flow, Environ, Sci. Technol, 55, 902-911.
- Woodley, A.L., Drury, C.F., Reynolds, W.D., Tan, C.S., Yang, X.M., Oloya, T.O., 2018. Longterm cropping effects on partitioning of water flow and nitrate loss between surface runoff and tile drainage. J. Environ. Qual. 47, 820–829. Xie, J., Liu, X., Wang, K., Yang, T., Liang, K., Liu, C., 2020. Evaluation of typical methods for
- baseflow separation in the contiguous United States. J. Hydrol. 583, 124628.
- Yue, F.-J., Waldron, S., Li, S.-L., Wang, Z.-J., Zeng, J., Xu, S., Zhang, Z.-C., Oliver, D.M., 2019. Land use interacts with changes in catchment hydrology to generate chronic nitrate pollution in karst waters and strong seasonality in excess nitrate export. Sci. Total Environ, 696, 134062.
- Zamyadi, A., Gallichand, J., Duchemin, M., 2007. Comparison of methods for estimating sediment and nitrogen loads from a small agricultural watershed. Can. Biosyst. Eng.
- Zimmer, M.A., Pellerin, B., Burns, D.A., Petrochenkov, G., 2019. Temporal variability in nitrate-discharge relationships in large rivers as revealed by high-frequency data. Water Resour. Res. 55, 973-989.